Projectile charge effects on the differential cross sections for the ionization of molecular nitrogen by positron and electron

G. Purohit[1,2] and D. Kato[1,3,4]

[1]National Institute for Fusion Science, National Institutes of Natural Sciences 322-6 Oroshi-cho, Toki Gifu, 509-5292, Japan
[2]Department of Physics, Sir Padampat Singhania University, Bhatewar, Udaipur-313601, India
[3]Department of Fusion Science, SOKENDAI, 322-6 Oroshi-cho, Toki Gifu, 509-5292, Japan
[4]Department of Advanced Energy Engineering, Kyushu University, Kasuga Fukuoka, 816-8580, Japan

Abstract

Triply differential cross sections (TDCS) are reported for the positron and electron impact ionization of molecular nitrogen at 250 eV projectile energy. The TDCSs have been calculated in the distorted wave Born approximation formalism using the orientation averaged molecular orbitals. The present attempt is helpful to analyze the recent measurements [Phys. Rev. A **93**, 032710 (2016)] and study the effect of projectile charge in the ionization of molecular target. The TDCS trends are compared for the positron and electron impact ionization in terms of binary and recoil intensities, binary lobe positions for different values of energy loss. The binary emission of electron is enhanced for positron impact however the nearly same recoil emission is observed for positron as well as electron impact. Significant discrepancies are observed from the measurements in terms of relative binary intensity for positron and electron impact.

I. Introduction

Ionization of atoms and molecules by electron impact has been studied since the initial experimental work [1] with a special emphasis on the study of triple differential cross section (TDCS), which provides important information about the collision dynamics. Later, the complete kinematics of the ionization process during and after the collision has been learnt through the powerful experimental techniques; Cold Target Recoil Ion Momentum Spectroscopy (COLTRIM) [2] and Recoil-ion Momentum Spectroscopy (RMS) [3]. Many of the experimental efforts have been for the atomic targets, mostly inert gases [4]. From last few years there has been growing interest to investigate the collision dynamics of molecular targets. The closely spaced energy levels of different molecular states and the orientation of the molecule make it difficult to measure the TDCS and it is also challenging for the theoretical models to describe the molecular ionization due to multi-center nature of the target wave functions. Despite of this, TDCS studies have been done for the molecular targets ranging from simple diatomic molecules to more complex molecules, few may be listed as H_2 [5-7], N_2 [8-13], O_2 [14], H_2O [15-17], CH_4 [18-20], HCOOH [21]. Complex molecules of biological interest such as DNA analogues [22], pyrimidine [23], thymine [24] etc. have also been investigated. Distorted wave and time-dependent close coupling approaches have been used to calculate the cross sections for the molecular hydrogen target and both the approaches have been successful to describe the features of TDCS [5, 25-26]. Variants of distorted wave formalism have been applied for the electron impact ionization of various molecular targets (see [27] and references cited in) and mixed degree of agreement has been achieved with the measurements, most of the time good agreement in the binary lobe region with certain discrepancies in the recoil scattering description [9].

Recently ionization by antiparticle impact such as positrons has been studied experimentally as well as theoretically. Such type of studies are helpful to understand the similarities or differences between antiparticle-matter and particle-matter interactions and are also helpful to obtain certain information which cannot be obtained only by the study of electron impact processes [28-29]. Differential studies with positrons are desirable to understand the collision dynamics in comparison with projectiles such as electrons or protons of same energy as well as to probe the effect of projectile charge and mass on the collision dynamics. Due to technical problem of low signal intensities the measurements for positron impact differential cross sections

have been less in comparison to the electron impact. To begin with single differential [30] and double differential cross sections [31-32] have been reported for the positron impact ionization. In few later attempts more single and double differential cross section results for the positron impact single as well as double ionization were obtained [33-34]. Various theoretical efforts have been made to study the positron impact ionization of atomic hydrogen [35-38]. Structures in the triply and doubly differential ionization cross sections of atomic hydrogen have been identified [35] and the cross sections have been found to depend on the description of three-body system [35-36]. The ionization of atomic hydrogen by fast positrons has been studied in the presence of laser field [37] and recently study based on two center approach to fully differential positron impact ionization of hydrogen has been reported [38].

First triple differential cross sections were measured for the positron impact ionization of argon atoms in coincidence with both the outgoing particles moving in forward direction [39]. Results of TDCS with wider range of emission angles have been reported for argon atoms [40-42]. Theoretical efforts based on the distorted wave formalism tried to analyze the differential cross section trends of positron impact ionization for the measurements reported [43-44]. Recent review details the progress and methods used in studying the inelastic interactions between positrons and atoms [45].

In the last decade, there has been increased interest to investigate the positron impact collision dynamics of molecular targets with emphasis on obtaining the information which are inaccessible by the study of electron impact only. There have been few attempts to measure positron impact fully differential cross sections for molecular targets. Triply differential study of positron impact ionization of H_2 molecules have been reported for the forward emission of scattered and ejected particles [46-47]. These efforts also verified the presence of broad peak in the ejected electron spectrum attributed to the process referred as electron capture to the continuum (ECC). Very recently de Lucio and DuBois [12] reported the triply differential cross section measurements for the positron and electron impact ionization of nitrogen molecules at 250 eV projectile energy. Apart from the recent experimental study [12], no other study is available for the positron and electron induced differential cross sections for N_2 molecules at same kinematical conditions, however electron impact TDCSs have been measured for the nearly same projectile energy [13]. Further to mention that, total cross sections have been calculated for the positron [48] and electron impact [49] ionization of N_2 molecule in the distorted wave

Born approximation (DWBA) approach and reasonable degree of agreement has been obtained with the measurements.

We report the triple differential cross section (TDCS) results for the positron and electron impact ionization of nitrogen molecule at 250 eV projectile energy. We analyze the recent measurements [12] reported to study the projectile charge effect in the ionization of molecular nitrogen, following which no theoretical results are available to compare, to the best of our knowledge. We also calculate and compare the electron impact TDCS for ionization of N_2 molecules for the kinematical conditions of earlier measurements [13] in the nearly same energy regime (incident energy ≈300 eV) as the recent measurements [12]. TDCSs have been calculated in the distorted wave Born approach using the orientation averaged molecular orbital approximation, the atomic units ($\hbar = e = m_e = 1$) have been used.

II. Theory

The positron and electron induced TDCS may be written in the following form:

$$\frac{d^3\sigma}{d\Omega_1\, d\Omega_2\, dE_1} = (2\pi)^4 \frac{k_1 k_2}{k_0} \sum_{av} |T(k_1, k_2, k_0)|^2 \quad . \tag{1}$$

A projectile with energy E_0 and momentum k_0 collides with the target molecule and produces scattered and ejected particles with energies E_1, E_2 and momenta k_1 , k_2 respectively in the outgoing channel, which are observed in coincidence. The energy conservation $E_0 = E_1+E_2+IP$ is followed, where IP is ionization potential of the target orbital. The transition matrix element (T) may be expressed in terms of the direct and exchange scattering amplitudes as;

$$|T|^2 = |f_{dir}|^2 + |f_{ex}|^2 - Re\left(f_{dir}^* f_{ex}\right) \tag{2}$$

where

$$f_{dir} = \left\langle X_1(k_1, r_1)\, X_2(k_2, r_2) \left| -\frac{Z}{r_{12}} \right| \psi^{OA}(r_2) X_0(k_0, r_1) \right\rangle \tag{3}$$

$$f_{ex} = \left\langle X_1(k_1, r_2)\, X_2(k_2, r_1) \left| -\frac{Z}{r_{12}} \right| \psi^{OA}(r_2) X_2(k_0, r_1) \right\rangle \tag{4}$$

here $Z = \pm 1$ is the charge of projectile ("+" for positron and "-" for electron). The incident particle is described by the distorted wave $X_0(k_0, r_1)$ and $X_1(k_1, r_1)$; $X_2(k_2, r_2)$ are the distorted wave-functions used for the scattered and ejected particles respectively, the particles 1 and 2 are exchanged in the expression of exchange amplitude (eq. 4). $\psi^{OA}(r_2)$ is the initial bound state wave function for the molecular target which is approximated as the orientation averaged molecular orbital for the orbitals of N_2 molecule. The molecular wave functions have been calculated using the density functional theory with B3LYP/TZ2P basis set [50].

The initial state distorting potential representing the interaction between projectile and target molecular electrons constitutes the contribution from molecular nuclei and a spherical symmetric potential obtained by averaging over all orientations using B3LYP basis sets. The molecular charge density for the neutral molecule is obtained by

$$\rho(r, R) = \sum_{k=1}^{m} n_k \left| \psi^{OA}(r, R) \right|^2 \tag{5}$$

where 'm' is the number of orbitals in the molecule and 'n_k' is the occupation number of the orbital. The average radial charge density is obtained by averaging eq. (5) over all orientations;

$\rho^{av}(r) = \langle \rho(r, R) \rangle$.

The spherically symmetric static distorting potential is then obtained using the average radial charge density

$$U_{el}(r_1) = \left\langle \int \frac{\rho^{av}(r) dr}{|r_1 - r|} \right\rangle . \tag{6}$$

We also calculate the TDCS using Coulomb potential in place of spherically symmetric potential of Eq. (6) for the smallest ejected electron energy (E_2 = 6 eV) to see the differences in the trends of TDCS.

As described above, the initial state static distorting potential is the sum of electronic contribution and nuclear contribution, i.e. $U_{static} = U_{el} + U_{nuc}$. The nuclear contribution (U_{nuc}) is obtained by placing the nuclear charge on a spherical cell having radius equal to the distance of nucleus from center of mass. The final state distorted potential is generated in the similar way constituting the nuclear contribution and spherically symmetric potential generated in the field of molecular ion. In addition to the static distorting potential the exchange distorting potential of

Furness and McCarthy [51], corrected by Riley and Truhlar [52] has been used to generate the total distorting potential;

$$U_E(r) = 0.5[E_0 - U_{static}(r) - \{[E_0 - U_{static}(r)]^2 + 4\pi\rho(r)\}^{1/2}]. \quad (7)$$

For the positron impact ionization there is no exchange amplitude f_{ex} and following choices have been made. The distorted waves for the incident $X_0(k_0, r_1)$ and scattered $X_1(k_1, r_1)$ positrons are generated in the static potential of the molecular target, the distorted waves for the ejected electron $X_2(k_2, r_2)$ is generated in the static exchange potential of the molecular ion.

In order to see the effect of screening the TDCSs have been calculated for the scattered particle in both the atomic potential and ionic potential, however the ejected electron is treated in the potential of residual ion in both cases. For the lowest ejected electron energy case (E_2 = 6 eV) the TDCSs have also been calculated by including correlation-polarization potential $V_{CP}(r)$ in the distorting potential. The correlation-polarization potential $V_{CP}(r)$ is given as follows;

$$V_{CP}(r) = V_{SR}^{Corr}(r), \quad r \le r_0$$
$$= -\frac{\alpha_d}{2r^4}, \qquad r > r_0 \quad (8)$$

where the fundamental form of the short range correlation and long range polarization potential has been approximated by means of local density functional theory [53, 54]. α_d is dipole polarizability of the target and $V_{SR}^{Corr}(r)$ is short range correlation potential [53]. The point r_0 is the intersection of the short range correlation and long range polarization potential, we have ensured the smooth matching of potentials at r_0.

The Coulomb interaction between the two outgoing particles has been treated by the Ward-Macek approximation [55], which has been found to give good agreement with the experimental data at lower energies and also reduces the computational difficulty [56].

The Ward-Macek factor is given by

$$M_{ee} = N_{ee}\left|{}_1F_1(-i\lambda_3, 1, -2ik_3 r_{3ave})\right|^2 \quad (9)$$

Where $N_{ee} = \frac{\gamma}{e^{\gamma} - 1}$ is the Gamow factor, $\gamma = -\frac{2\pi}{|k_1 - k_2|}$

$$\lambda_3 = -\frac{1}{|k_1 - k_2|} \text{ and } r_{3ave} = \frac{\pi^2}{16\varepsilon}\left(1 + \frac{0.627}{\pi}\sqrt{\varepsilon}\ln\varepsilon\right)^2 . \quad (9)$$

ε is the total energy of the two exiting electrons. The sign of γ and λ_3 are changed for the PCI calculation of positron impact.

The DWBA formalism along with the orientation averaged molecular orbital approximation is capable to produce reliable TDCS results at the incident electron energy 250 eV used in the present study [11, 56]. The DWBA has been very successful at the higher energies [9], however the DWBA with PCI effects have been found successful at the intermediate energies also [56]. The DWBA is useful in describing the complex multicenter and multi-orientation problem of molecular ionization as it can be applied for any energy and any size molecule and effects such as PCI makes it suitable for the lower energies also [56]. The orientation averaged molecular orbital approximation used in the present investigation has been found to be successful for the symmetric molecular states (see [56] and references cited in) and is useful to give the first estimates for the positron impact ionization of molecular nitrogen, however the calculation with proper average over all orientations of molecular target using DWBA formalism is computationally challenging.

III. Results and Discussion

The triply differential cross section (TDCS) measurements for the positron impact ionization of nitrogen molecules have been reported for the first time [12]. The measurements of electron impact TDCSs are also reported for the same kinematical conditions and the trends of TDCSs obtained through the experimental study for positron and electron ionization of nitrogen molecules are compared in terms of relative binary and recoil peak intensities, relative positions of binary peaks. We report the results of TDCS for the positron and electron impact ionization of molecular nitrogen for the same kinematical conditions used in the recent measurements [12]. The TDCSs have been calculated in the distorted wave Born approach using the orientation averaged molecular orbital approximation for the ionization taking place from the $3\sigma_g$ orbital of N_2.

The TDCS results are presented at projectile energy 250 eV for different average ejected electron energies at scattering angle 3^0, through which the TDCS information is obtained for the momentum transfer ranging from 0.27 to 0.44 a.u. The calculated TDCSs have been compared with the corresponding measurements. The TDCS results are displayed for ejected electron energy 12.4 eV in Figure 1. The solid curve in Fig 1(a) is plot for the positron impact ionization and the solid curve in Fig. 1(b) is plot for the electron impact ionization, the scattered particle is treated in ion potential in both cases. The dashed curves in both the frames are for the scattered particles treated in atom potential. The solid red circles (Fig. 1a) and solid black circles (Fig. 1b) are the experimental TDCS [12] for the positron and electron impact ionization respectively. The measurements have been normalized to the positron TDCS (solid curve in Fig. 1a) in the binary peak region for best visual fit while retaining relative normalization between electron and positron impact. Binary and recoil regions are identified in the TDCS results, experimentally as well as theoretically. The binary peak positions observed in the theoretical TDCS for the positron as well as electron case are shifted towards lower values of ejected electron angle in comparison to the measurements. It is observed that the binary electron emission is enhanced for the positron impact ionization, which is similar as shown by the measurements. However, there are discrepancies between theoretical results and measurements in the relative magnitude of binary peak for positron and electron case. The recoil emission of electron is decreased for the positron impact ionization in the calculations; in contrast to this the measurements have recoil peak intensity slightly higher for positron impact case.

The TDCS results calculated at ejected electron energies 6.0 eV and 24.7 eV are presented in Figure 2. These calculations have been done at scattering angle 3^0 for momentum transfer 0.29 a.u. (Fig. 2a) and 0.42 a.u. (Fig. 2b). The calculated TDCS results have been compared with the fits to the individual data obtained by [12] for best visual fit while retaining relative normalization between electron and positron impact. At the small momentum transfer case (Fig. 2a) a large recoil peak is observed for both the positron and electron impact ionization in the DWBA results, however still retaining the nature of trends; enhanced binary peak and smaller recoil peak for the positron impact. The positron recoil peak in the calculated results is slightly higher than electron impact at larger momentum transfer (Fig. 2b). The TDCS curves with and without PCI are plotted for both the electron and positron impact case, the PCI has not been found to change the trends of TDCS significantly with changes less than 1% (see the black solid

and black dashed curves in Fig. 2a). For the higher momentum transfer (Fig. 2b) the recoil peaks for the positron and electron impact ionization are of nearly same intensities, which are also observed by the measurements. As observed previously there is certain discrepancy in the theoretical results and measurements in terms of relative height of binary peaks for positron and electron impact and also in terms of position of peaks.

We have also calculated TDCS for the ionization of N_2 molecules using Coulomb potential in place of the spherically symmetric potential of Eq. (6) and including correlation-polarization potential in the distorting potential. We observe that using different forms of potentials do not change the trends of TDCS significantly for both the electron as well as positron impact ionization. The main discrepancy in the relative magnitude of binary peak for the electron and positron impact still remains same. Changes in the magnitudes of TDCS are observed, the plots including different forms of potentials are presented in Figure 3 for the lowest ejected electron energy used in present study (E_2 = 6 eV). The three outer $3\sigma_g, 1\pi_u$ and $2\sigma_u$ valence orbitals of nitrogen molecules have very near values of ionization potentials. We have calculated the TDCS for the contribution from these individual orbitals at ejected electron energy 12.4 eV (Figures 4a, 4b) and 6.0 eV (Figures 4c, 4d). We observe that the major contribution to TDCS for both the electron and positron impact is from $3\sigma_g$ orbital. The TDCS calculated for the $2\sigma_u$ orbital has larger binary peak and smaller recoil peak however both the $3\sigma_g, 1\pi_u$ orbital TDCSs have larger recoil and smaller binary peak ratio.

The discrepancies in the binary peak positions and the intensities of binary and recoil lobes are better visualized through the comparison shown in Figure 5, between the theoretical results and the measurements. The direction of binary lobes for 250 eV positron and electron ionization of molecular nitrogen are plotted as a function of momentum transfer in Figure 5(a). The momentum transfer considered is ranging from 0.27 a.u. to 0.44 a.u. corresponding to various energy loss cases considered in the measurements [12]. The blue solid triangles and red solid circles are the experimental positions of binary lobes for electron impact and positron impact respectively. The red solid line and blue dashed line are the binary positions observed by present calculations for positron and electron impact respectively. The black dotted line is the binary peak positions calculated according to the kinematic conditions. An addition of 10^0 angle has been made in the theoretical binary peak positions for better comparison with measurements.

The binary peak positions in the measurements are shifted towards higher values of ejected electron angle in comparison to the directions predicted by theoretical results. The binary peak in the measurements for electron impact is at higher ejected electron angle in comparison to positron impact except few cases, however the present theoretical results show that the binary lobe for positron impact is observed at higher ejected electron angles (solid red line in Fig. 5a).

The experimental and theoretical values for the maximum binary and recoil intensities are also compared as a function of momentum transfer in Figure 5(b). Both the experiments and theoretical results show the increased binary emission of electron for positron impact ionization (the solid red triangles and solid red line), however the theoretical relative intensity of binary peak for electron impact is not as less as reported by the measurements (the blue solid line and blue solid triangles). The measurements also show a higher recoil emission of electron for positron impact ionization (hollow solid circles), the theoretical results show slightly higher recoil peak intensity for electron impact for smaller momentum transfer (dashed red line).

We have also calculated TDCS for the electron impact ionization taking place from the $3\sigma_g$ orbital of nitrogen molecule for the kinematical conditions of earlier measurements [13], following which there are no other theoretical results available to compare to the best of our knowledge. The DWBA results with OAMO are reported for the ejected electron energies 10 eV (Figure 6a, 6b) and 18.4 eV (Figure 6c, 6d) and compared with the measurements [13]. The measurements have been normalized to theoretical results for the best visual fit. The binary peak for all the cases overestimate the experimental binary peak, however the binary to recoil peak ratio improves at higher values of scattering angles. The experimental and theoretical peak positions agree reasonably well except Fig. 6c.

The differences in the trends of TDCS for the positron and electron impact ionization of nitrogen molecules are attributed to mainly the exchange term in the Hamiltonian due to charge of projectile. For the electron case there is exchange in the elastic scattering in the incident channel and for the both the outgoing electrons also. The exchange amplitude is calculated and included in the calculation of TDCS. For the case of positron impact there is no exchange amplitude and the distorted waves for the positron are generated in the static potential of the nitrogen molecule, however the distorted wave for the ejected electron is calculated in the static-exchange potential of the molecular ion. The post collision interaction (PCI) is included using the WM factor for both the electron and positron impact cases, the PCI is of opposite sign for positron case due to

positron and electron in the outgoing channel. The role of PCI has not been found significant for kinematics of the present calculations for both the electron as well as positron impact cases so the exchange is the dominant effect responsible for the different trends of TDCS observed. The TDCS curves including PCI and without PCI are plotted in Figure 2a for the smallest ejected electron energy which show that the inclusion of PCI does not make significant change in the trends of TDCS. We have calculated TDCS using atom potential as well as ion potential for the scattered particle (Figure 1) as the scattered particle is faster than the ejected electron in the kinematics used presently. Shift of the binary peak position towards higher ejected electron angle and increase of magnitude is observed for the TDCS calculated in the ion potential for the scattered particle.

The description of fully differential cross section for electron impact ionization of molecular target is still an open problem and there are many un-answered questions. The theoretical formalism used till date are basically based on the variants of distorted waves approach using orientation averaged methods to describe the molecular target states, only few non perturbative attempts has been made for hydrogen molecule [25-26]. Present attempt is able to describe the trends of TDCS for positron and electron impact ionization of nitrogen molecules up to some extent with points of agreement and disagreement with the measurements. The prime disagreement lies in the relative magnitude of binary peak for the electron impact and the peak positions. Larger binary peaks are observed in the present calculations for the electron impact ionization which disagree with the measurements [12, 13]. The OAMO method used in the present study has been found to be successful for the molecules such as H_2 and N_2 [11, 55], particularly at the smaller momentum transfer conditions below unity. The results obtained for the kinematics of present study have large degree of disagreement as described above. We have also calculated TDCS using Coulomb potential as well as addition of polarization potential in the distorting potential however the trends of TDCS have not varied significantly. The TDCS have also been calculated to see the contribution of TDCS from the ionization of other valence orbitals of nitrogen molecules, however the relative binary peak intensity for positron and electron impact is not observed as in the measurements [12]. The disagreement with the measurements in terms of binary to recoil peak ratio may be due to second order effects, particularly at the lower ejected electron energies. The other possible reason for large discrepancies may be the use of orientation averaged molecular orbital. The proper average (PA) over orientation-dependent

cross-sections may be the other option which has been recently found to give better agreement with the measurements for H_2O molecules [57], however the computational cost of proper average method is exceptionally high requiring more than thousand processors. Calculations in the second order Born approximation may also be tested in future. In absence of any other theoretical results for analysis of the measurements [12, 13] and the large uncertainty in the measurements reported (authors of [12] already cautioned for comparison on absolute scale and authors of [13] have mentioned uncertainties in the absolute scale), the present effort in the OAMO may give the predictions of theoretical TDCSs and provoke further theoretical attempts with other forms of approximation such as PA as well as considering the second order Born term.

IV. Conclusions

In conclusion, present study gives insight of the positron and electron impact interactions with the molecular nitrogen and the effect of the exchange term in the Hamiltonian due to the sign of projectile on the collision dynamics. The trends of TDCS are extracted as a function of momentum transfer through various energy loss values. The effect of reversal of the direction of Coulomb field between the projectile and molecular target is studied through the relative intensities of binary lobe for positron and electron impact and the directions of the binary lobes. There are points of agreement and disagreement between the theoretical and experimental results with large discrepancies. Both the theory and measurements show enhanced binary emission of electron for positron impact ionization. Nearly same recoil intensities for positron and electron impact are observed for the higher momentum transfer both in the theoretical and experimental results. There are significant discrepancies in the relative magnitude of binary lobes for electron impact case. The binary lobe positions obtained by the theoretical results are shifted towards lower values of ejected electron angles in comparison to the experimental positions. TDCSs have also been calculated with different forms of interaction potential and TDCS contributions from other valence orbitals have also been investigated however the prime discrepancy of overestimated binary peaks for electron impact is not resolved. Future efforts with second order distorted wave Born approximation and proper average may be useful to further investigate the trends of TDCS for the N_2 molecules in comparison with the available measurements.

Acknowledgments

We wish to thank Dr. Chuangang Ning for help in calculating B3LYP basis sets. We also thank Prof. Don Madison for useful suggestions. GP acknowledges JSPS Long Term Fellowship AY 2017 (L17538) provided by Japan Society for Promotion of Science. GP also acknowledges National Institute for Fusion Science (NIFS), Toki Japan for providing hospitality and Sir Padampat Singhania University (SPSU), Udaipur, India for providing sabbatical leave.

References:

[1] H. Ehrhardt, M. Schulz, T. Tekaat and K. Willmann, Phys. Rev. Lett. **22**, 89 (1969).
[2] R. Dorner, V. Mergel, O. Jagutzki, L. Spielberger, J. Ullrich, R. Moshammer and H. Schmidt-Bocking, Phys. Rep. **330**, 95 (2000).
[3] J. Ullrich, R. Moshammer, R. Dorner, O. Jagutzki, V. Mergel, H. Schmidt-Bocking and L. Spielberger, J. Phys. B: At. Mol. Opt. Phys. **30**, 2917 (1997).
[4] A. Naja, E. M. Staicu Casagrande, A. Lahmam-Bennani, M. Stevensson, B. Lohmann, C. Dal Cappello, K. Bartschat, A. kheifets, I. Bray and D. V. Fursa, J. Phys. B: At. Mol. Opt. Phys. **41**, 085205 (2008).
[5] O. Al-Hagan, C. Kaiser, D. H. Madison and A. J. Murray, Nat. Phys. **5**, 59 (2010).
[6] A. Senftleben, T. Pflueger, X. Ren, O. Al-Hagan, B. Najjari, D. Madison, A. Dorn and J. Ullrich, J. Phys. B **43**, 081002 (2010).
[7] D. S. Milne-Brownile, M. Foster, J. Gao, B. Lohmann and D. H. Madison, Phys. Rev. Lett. **96**, 233201 (2006).
[8] L. R. Hargreaves, C. Coyler, M. A. Stevenson, B. Lohmann, O. Al-Hagan, D. H. Madison and C. G. Ning, Phys. Rev. A **80**, 062704 (2009).
[9] A. Lahmam-Bennani, E. M. Staicu Casagrande and A. Naja, J. Phys. B **42**, 235205 (2009).
[10] A. J. Murray, M. J. Hussey, I. Bray, J. Gao and D. H. Madison, J. Phys. B **39**, 3945 (2006).
[11] H. Chaluvadi, Z. N. Ozer, M. Dogan, C. Ning, J. Colgan and D. Madison, J. Phys. B: At. Mol. Opt. Phys. **48**,155203 (2015).
[12] O. G. de Lucio and R. D. DuBois, Phys. Rev. A **93**, 032710 (2016).
[13] L. Avaldi, R. Camilloni, E. Fainelli and G. Stefani, J. Phys. B: At. Mol. Opt. Phys. **25**, 3551 (1992).
[14] J. Yang and J. P. Doering, Phys. Rev. A **63**, 032717 (2001).
[15] K. L. Nixon, A. J. Murray, O. Al-Hagan, D. H. Madison and C. Ning, J. Phys. B **43**, 035201 (2010).
[16] C. Kaiser, D. Spieker, J. Gao, M. Hussey, A. Murray and D. H. Madison, J. Phys. B **40**, 2563 (2007).
[17] L. Fernández-Menchero and S. Otranto, J. Phys. B: At. Mol. Opt. Phys. **47,** 035205 (2014).
[18] H. Chaluvadi, C. G. Ning and D. H. Madison, Phys. Rev. A. **89**, 062712 (2014).
[19] K. L. Nixon, A. J. Murray, H. Chaluvadi, S. Amami, D. H. Madison and C. G. Ning, J. Chem. Phys. **136**, 094302 (2012).
[20] L. Fernández-Menchero and S. Otranto, Phys. Rev. A **82**, 022712 (2010).

[21] C J Colyer, M A Stevenson, O Al-Hagan, D H Madison, C G Ning and B Lohmann, J. Phys. B: At. Mol. Opt. Phys. **42**, 235207 (2009).
[22] D.B. Jones, J.D. Builth-Williams, S.M. Bellm, L. Chiari, H. Chaluvadi, D.H. Madison, C.G. Ning, B. Lohmann, O. Ingólfsson and M.J. Brunger, Chem. Phys. Lett. **572**,32 (2013).
[23] J. D. Builth-Williams, S. M. Belim, D. B. Jones, H. Chaluvadi, D. H. Madison, C. G. Ning, B. Lohmann and M. J. Mrunger, J. Chem. Phys. **136**, 024304 (2012).
[24] S. M. Bellm, C. J. Coyler, B. Lohmann and C. Champion, Phys. Rev. A **85**, 022710 (2012).
[25] J. Colgan, M. S. Pindzola, F. Robicheaux, C. Kaiser, A. J. Murray and D. H. Madison, Phys. Rev. Lett. **101**, 233201 (2008).
[26] J. Colgan, O. Al-Hagan, D. H. Madison, C. Kaiser, A. J. Murray, M. S. Pindzola, Phys. Rev. A **79**, 052704 (2009).
[27] E. Ali, K. Nixon, A. J. Murray, C. G. Ning, J. Colgan and D. Madison, Phys. Rev. A **92**, 042711 (2015).
[28] G. Laricchia, S. Armitage, A. Kover, D. J. Murtagh, Adv. At. Mol. Opt. Phys. **56**, 1 (2008).
[29] M. Mc Govern, D. Assafrao, J. R. Mohallem, C. T. Whelan, H. R. J. Walters, Phys. Rev. A **79**, 042707 (2009).
[30] J. Moxom, G. Laricchia, M. Charlton, G. O. Jones and A. Kover, J. Phys. B: At. Mol. Opt. Phys. **25**, L613 (1992).
[31] A. Schmitt, U. Cerny, H. Moller, W. Raith and M. Weber, Phys. Rev. A **49**, R5(R) (1994).
[32] R. D. DuBois, C. Doudna, C. Lloyd, M. Kahveci, K. Khayyat, Y. Zhou and D. H. Madison, J. Phs. B: At. Mol. Opt. Phys. **34**, L783 (2001).
[33] A. C. F. Santos, A. Hasan, T. Yates and R. D. DuBois, Phys. Rev. A **67**, 052708 (2003).
[34] A. C. F. Santos, A. Hasan and R. D. DuBois, Phys. Rev. A **69**, 032706 (2004).
[35] J. Berakdar and H. Klar, J. Phys. B: At. Mol. Opt. Phys. **26**, 3891 (1993).
[36] J. Fiol and R. E. Olson, J. Phys. B: At. Mol. Opt. Phys. **35**, 1173 (2002).
[37] J. Pan, Shu-Min Li and J. Berakdar, Opt. Lett. **32**, 585 (2007).
[38] A. S. Kadyrov, J. J. Bailey, I. Bray and A. T. Stelbovics, Phys. Rev. A **89**, 012706 (2014).
[39] A. Kover, G. Laricchia and M. Charlton, J. Phys. B: At. Mol. Opt. Phys. **26**, L575 (1993).
[40] O. G. de Lucio, S. Otranto, R. E. Olson and R. D. DuBois, Phys. Rev. Lett **104**, 163201 (2010).
[41] O. G. de Lucio, J. Gavin and R. D. DuBois, Phys. Rev. Lett. **97**, 243201 (2006).
[42] J. Gavin, O. G. de Lucio and R. D. DuBois, Phys. Rev. A **95**, 062703 (2017).
[43] R. I. Campeanu, H. R. J. Walters and C. T. Whelan, Eur. Phys. J. D **69**, 235 (2015).
[44] G. Purohit and D. Kato, Phys. Rev. A **96**, 042710 (2017).
[45] R. D. DuBois, J. Phys. B: At. Mol. Opt. Phys. **49**, 112002 (2016).
[46] A. Kover and G. Laricchia, Phys. Rev. Lett. **80**, 5309 (1998).
[47] C. Arcidiacono, A. Kover nd G. Laricchia, Phys. Rev. Lett. **95**, 223202 (2005).
[48] R. I. Campeanu, V. Chis, L. Nagy and A. D. Stauffer, Nucl. Instr. And Meth. In Phys. Res. B **221**, 21 (2004).
[49] I. Toth, R. I. Campeanu, V. Chis and L. Nagy, Eur. Phys. J D **48**, 351 (2008).
[50] C. Lee, W. Yang and R. G. Parr, Phys. Rev. B **37**, 785 (1988).

[51] J. B. Furness and I. E. McCarthy, J. Phys. B **6**, 2280 (1973).
[52] M. E. Riley and D. G. Truhlar, J. Chem. Phys. **63**, 2182 (1975).
[53] N. T. Padial and D. W. Norcross, Phys. Rev. A **29**, 1742 (1984).
[54] J. P. Perdew and A. Zunger, Phy. Rev. B **23**, 5048 (1981).
[55] S. J. Ward and J. H. Macek, Phys. Rev. A **49**, 1049 (1994).
[56] D. H. Madison and O. Al-Hagan, J. At. Mol. Opt. Phys. **2010**, 367180 (2010).
[57] X. Ren, S. Amami, K. Hossen, E. Ali, C. G. Ning, J. Colgan,D. H. Madison, and A. Dorn, Phys. Rev. A **95**, 022701 (2017).

Figure Captions

Figure 1: TDCS plotted as a function of ejected electron angle for the ionization of N_2 molecule at projectile energy 250 eV, ejected electron energy 12.4 eV and scattering angle 3^0 (a) positron impact ionization, red solid circles: measurements [12]; solid and dashed lines: DWBA results with scattered particle in ion and atom potential respectively (b) electron impact ionization, black solid circles: measurements [12]; solid and dashed lines: DWBA results with scattered particle in ion and atom potential respectively. Measurements have been normalized to positron curve for best visual fit while retaining relative normalization between electron and positron impact.

Figure 2: TDCS plotted as a function of ejected electron angle for the ionization of N_2 molecule at projectile energy 250 eV and scattering angle 3^0 (a) ejected electron energy 6.0 eV, black solid and red solid curves: DWBA results for positron with and without PCI respectively; black dashed and red dashed curves: DWBA results for electron with and without PCI respectively; red solid circles: fits to measurements [12] for positron impact and black solid circles: fits to measurements [12] for electron impact (b) ejected electron energy 24.7 eV, red solid and black dashed curves: DWBA results for positron and electron impact respectively, other legends are same as (a). Fits to measurements have been normalized to positron curve for best visual fit while retaining relative normalization between electron and positron impact.

Figure 3: TDCS plotted as a function of ejected electron angle for the ionization of N_2 molecule at projectile energy 250 eV, ejected electron energy 6.0 eV and scattering angle 3^0; red solid and red dashed curves: DWBA results for positron and electron impact in spherically symmetric averaged potential; black solid and black dashed curves: DWBA results for positron and electron impact in Coulomb potential; blue solid and blue dashed curves: DWBA results for positron and electron impact in spherically symmetric averaged potential with inclusion of polarization potential; red solid circles: fits to measurements [12] for positron impact and black solid circles: fits to measurements [12] for electron impact. Fits to measurements have been normalized to positron curve for best visual fit while retaining relative normalization between electron and positron impact.

Figure 4: TDCS plotted as a function of ejected electron angle for the ionization of N_2 molecule at projectile energy 250 eV from different orbitals; solid curve: $3\sigma_g$; dashed curve: $1\pi_u$; dotted curve: $2\sigma_u$ (a, c) positron impact and (b, d) electron impact; red solid circles: measurements (a) and fits to measurements (c) [12] for positron impact; black solid circles: measurements (b) and fits to measurements (d) [12] for electron impact. Measurements and fits to measurements have been normalized to solid black curve for positron impact for best visual fit while retaining relative normalization between electron and positron impact.

Figure 5: (a) Binary lobe angles plotted as a function of momentum transfer, red solid line and blue dashed line: present DWBA results with addition of 10^0 for positron and electron impact respectively; black dotted line: results calculated from kinematics; red solid circles: measurements [12] for positron impact and blue solid triangles: measurements [12] for electron impact (b) binary and recoil intensities plotted as a function of momentum transfer, red solid curve and red dashed curve: theoretical binary and recoil intensities for positron impact; blue solid curve and blue dashed curve: theoretical binary and recoil intensities for electron impact; red solid triangles and red hollow triangles: experimental binary and recoil intensities for positron impact [12]; blue solid triangles and blue hollow triangles: experimental binary and recoil intensities for electron impact [12]. Measurements for binary intensity have been normalized to the red solid curve for positron impact for best visual fit and the other measurements have been plotted retaining the relative normalization.

Figure 6: TDCS plotted as a function of ejected electron angle for the electron impact ionization of N_2 molecule. Solid curve: DWBA results with OAMO; black solid circles: measurements [13]. Measurements have been normalized to solid curve for best visual fit. Kinematics is displayed in each frame.

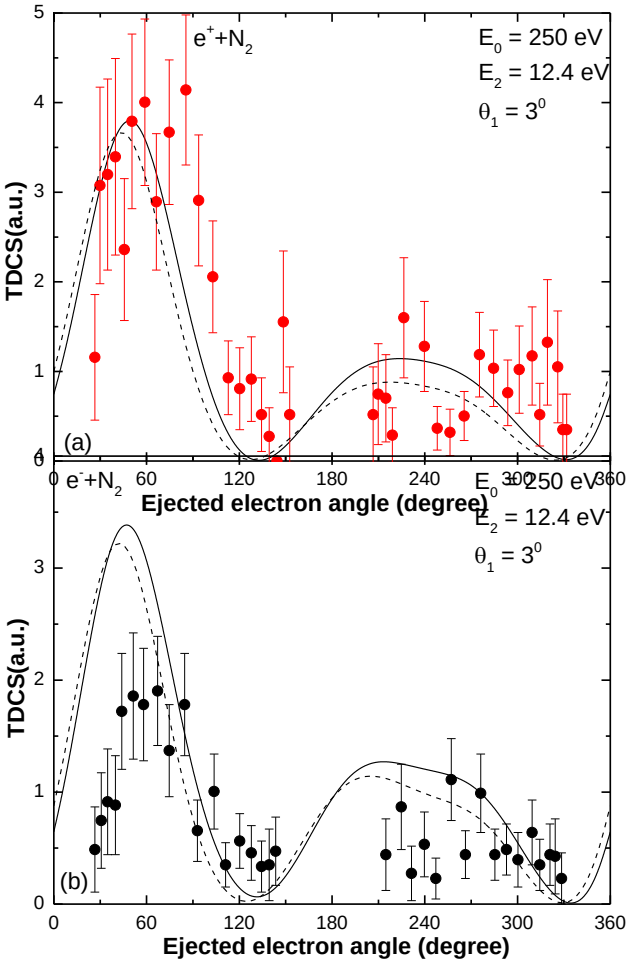
e+N2
E0 = 250 eV
E2 = 12.4 eV
θ1 = 30
TDCS(a.u.)
(a)
e-+N2
E0 = 250 eV
E2 = 12.4 eV
θ1 = 30
TDCS(a.u.)
(b)
Ejected electron angle (degree)
Ejected electron angle (degree)

Figure 1

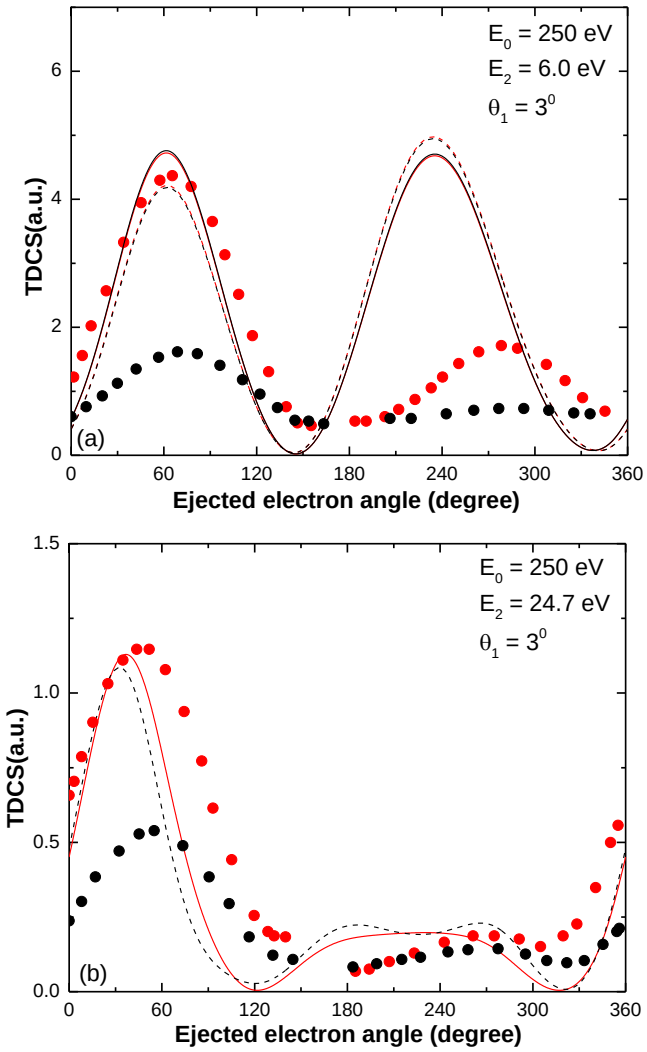
E0 = 250 eV
E2 = 6.0 eV
θ1 = 3^0
TDCS(a.u.)
(a)
Ejected electron angle (degree)
E0 = 250 eV
E2 = 24.7 eV
θ1 = 3^0
TDCS(a.u.)
(b)
Ejected electron angle (degree)

Figure 2

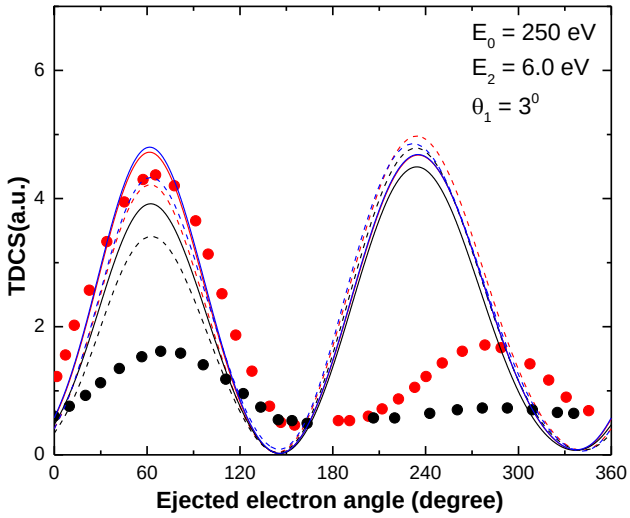
E0 = 250 eV
E2 = 6.0 eV
θ1 = 3^0
TDCS(a.u.)
Ejected electron angle (degree)
0
2
4
6
0
60
120
180
240
300
360

Figure 3

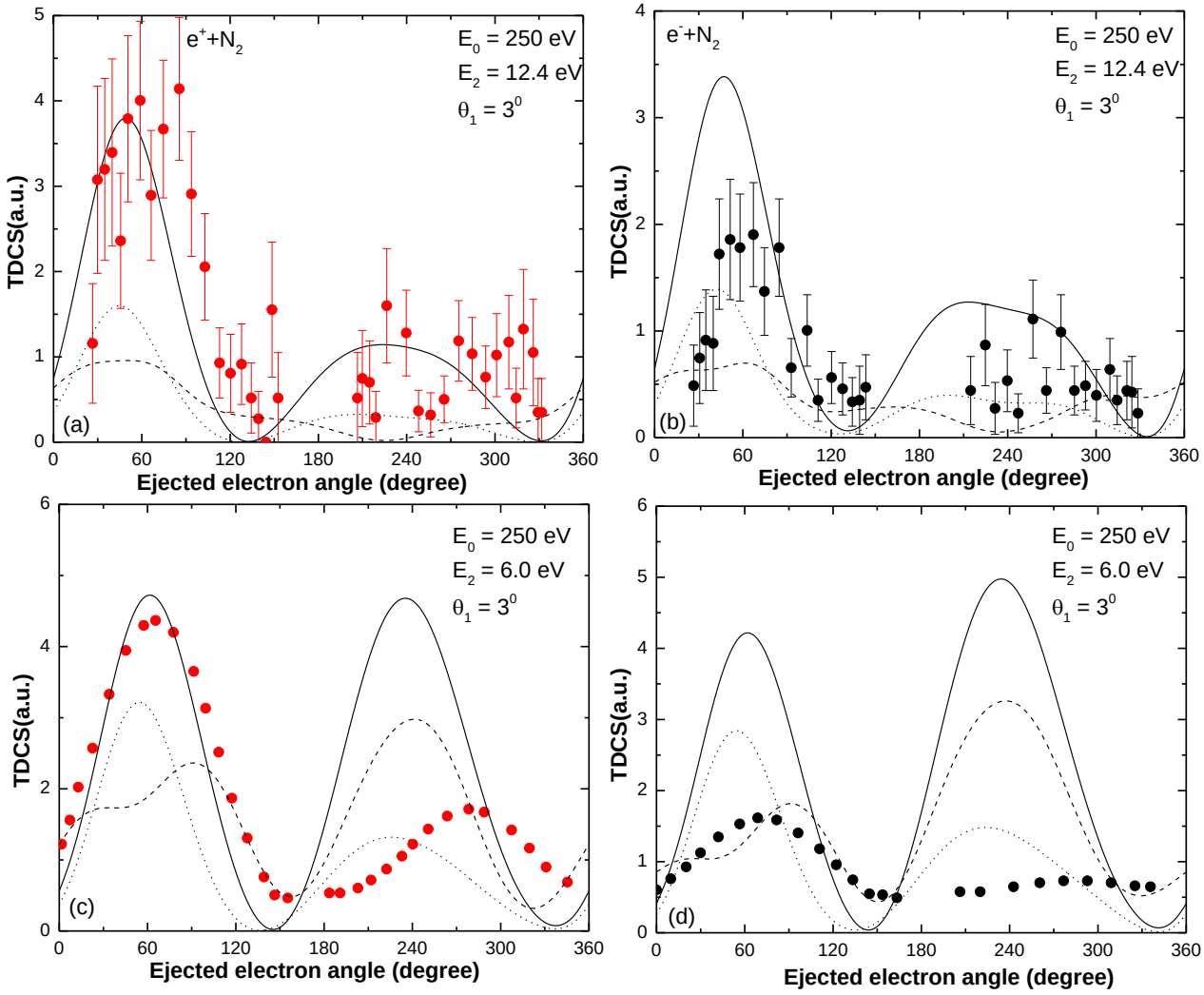
e+N2
E0 = 250 eV
E2 = 12.4 eV
θ1 = 30
(a)
TDCS(a.u.)
Ejected electron angle (degree)
e-N2
E0 = 250 eV
E2 = 12.4 eV
θ1 = 30
(b)
TDCS(a.u.)
Ejected electron angle (degree)
E0 = 250 eV
E2 = 6.0 eV
θ1 = 30
(c)
TDCS(a.u.)
Ejected electron angle (degree)
E0 = 250 eV
E2 = 6.0 eV
θ1 = 30
(d)
TDCS(a.u.)
Ejected electron angle (degree)

Figure 4

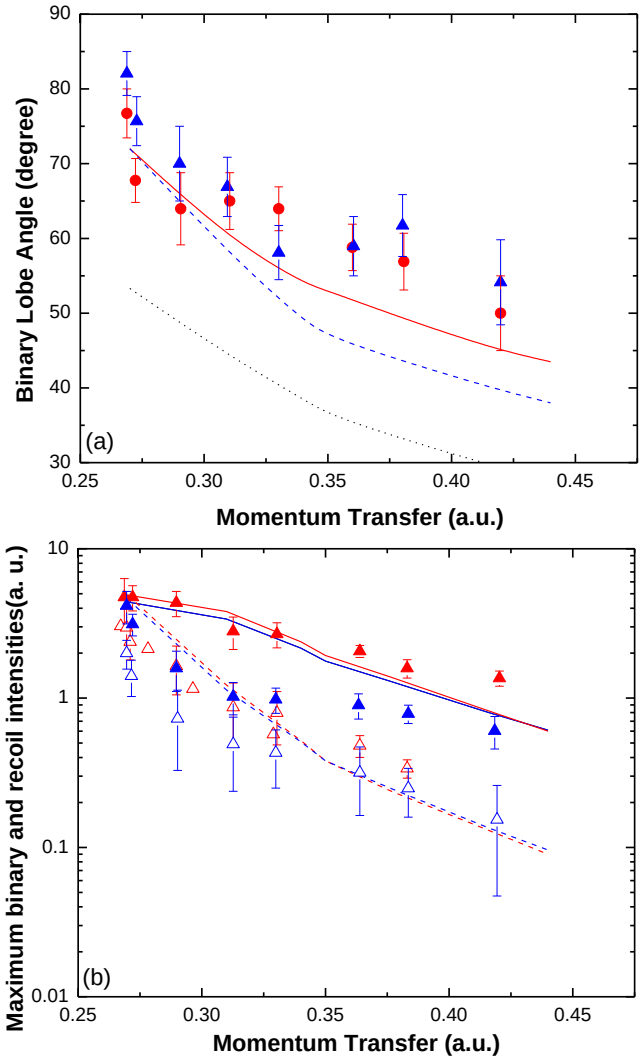
Binary Lobe Angle (degree)
90
80
70
60
50
40
30
(a)
0.25
0.30
0.35
0.40
0.45
Momentum Transfer (a.u.)
Maximum binary and recoil intensities(a. u.)
10
1
0.1
0.01
(b)
0.25
0.30
0.35
0.40
0.45
Momentum Transfer (a.u.)

Figure 5

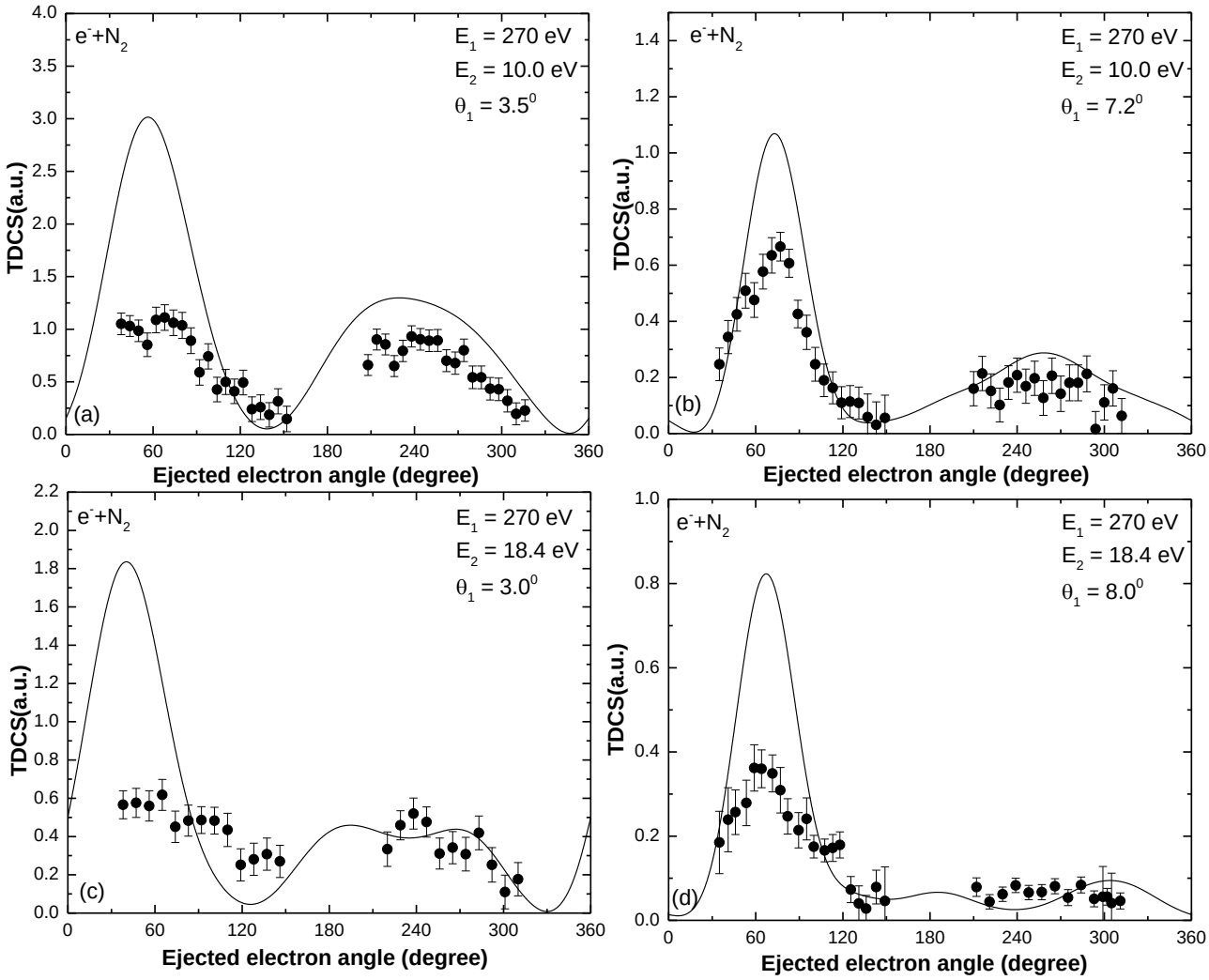
e-+N2
E1 = 270 eV
E2 = 10.0 eV
θ1 = 3.5^0
(a)
TDCS(a.u.)
Ejected electron angle (degree)
e-+N2
E1 = 270 eV
E2 = 10.0 eV
θ1 = 7.2^0
(b)
TDCS(a.u.)
Ejected electron angle (degree)
e-+N2
E1 = 270 eV
E2 = 18.4 eV
θ1 = 3.0^0
(c)
TDCS(a.u.)
Ejected electron angle (degree)
e-+N2
E1 = 270 eV
E2 = 18.4 eV
θ1 = 8.0^0
(d)
TDCS(a.u.)
Ejected electron angle (degree)

Figure 6